





Array Decomposition Method for Arbitrary-Element Regular Arrays Using Higher Order Basis Functions

Magnus Brandt-Møller , Michael Mattes , Olav Breinbjerg , *Fellow, IEEE*, Min Zhou , *Member, IEEE*, and Oscar Borries, *Member, IEEE*

Abstract—The full-wave array decomposition method for regular antenna arrays with arbitrary elements using higher order hierarchical basis functions is investigated. We show that the use of higher order basis functions results in significantly reduced memory consumption and computation time for a 10×10 element conical horn array with an aperture size of $22 \times 22\lambda$, without the need for analytical nor numerical approximations. In addition, we demonstrate that by employing higher order basis functions, the far-field error is considerably lower than by using common first-order basis functions for the same total number of unknowns.

Index Terms—Block Toeplitz (BT), finite arrays, full-wave, higher order (HO) basis functions (BF), higher order convergence.

I. INTRODUCTION

ANTENNA arrays have customarily been used as feeds for reflector-based systems and in radar applications. With the current trend to move from large spacecrafts in the geostationary orbit to smaller spacecrafts in low earth orbits, and a concurrent demand for flexible in-orbit configurations, electrically large direct radiating arrays (DRA) are becoming more frequently used for space missions. In this regard, traditional design approaches based on embedded element patterns and array factors or variants thereof have become inadequate, primarily due to their inaccurate modeling of edge and mutual coupling effects. For the typically more densely packed elements in DRA, it is important that mutual coupling effects are taken into account, which together with stringent performance requirements in space substantiates the necessity of rigorous full-wave numerical methods.

Traditional full-wave methods, e.g., the method of moments (MoM), suffer from excessive memory consumption and computational complexity, $\mathcal{O}(N^2)$ and $\mathcal{O}(N^2) - \mathcal{O}(N^3)$, respectively, where N is the number of unknowns. A range of methods have been proposed for more efficient analysis of electrically

large arrays, in which the memory consumption and computational complexity become $\mathcal{O}(N \log N)$. Examples include the multilevel fast multipole method (MLFMM) [1], [2], [3], the adaptive integral method [4], [5], the precorrected fast Fourier transform (FFT) [6], and variants hereof [7]. These methods are well suited to accelerate the analysis of general arrays. In the case of regular antenna arrays, the efficiency can be increased even further, both in terms of reduced memory consumption and computation time, by exploiting the regularity of the geometry [8].

The present work concerns the full-wave MoM solution of electrically large regular antenna arrays with arbitrary perfect electrically conducting (PEC) volumetric antenna elements, which is a common configuration for modern antenna arrays. Using the array decomposition method (ADM), the translational invariance of the free-space green function, together with the regular (e.g., rectangular, triangular, or circular) geometrical lattice of the array and a consecutive basis functions (BF) numbering, the resulting MoM matrix becomes multilevel block-Toeplitz (BT) [9], which allows for a FFT-accelerated matrix-vector product (MVP) [8], [10] in the iterative solver. It is, however, known that both the computation time and memory consumption of ADM scales as the square of the number of BF per array element [10]. Consequently, it is of interest to keep the number of BF as low as possible for a fixed solution accuracy. Several approaches have been proposed to reduce the quadratic dependency on the number of BF on each array element [8], [11]; they are, however, based on error-controllable approximations.

We demonstrate how the number of BF per array element can be reduced using hierarchical higher order (HO) BF [12], while retaining the desired solution accuracy. By using HO-BF in combination with ADM, a significant reduction in computation time and memory consumption can be achieved. Two test cases are used to demonstrate the benefits of HO BF. The HO-ADM is applied to a 10×10 ($22 \times 22\lambda$) conical horn array, resulting in much lower computation times compared with the ADM using first-order BF. We also apply HO-ADM to analyze the scattering from a 5×5 array of PEC spheres and look at the solution error as a function of the total number of unknowns. By increasing the polynomial order, the far-field solution error is considerably lower than by employing first-order BF, for the same total number of unknowns. We note that this is the first time, to the best of our knowledge, such HO convergence [13] has been demonstrated using the ADM in combination with hierarchical HO BF.

The rest of this letter is organized as follows. Section II outlines the mathematical foundation of the ADM. Section III reviews the employed BF and showcases HO convergence for an

Manuscript received 8 July 2022; revised 10 August 2022 and 15 August 2022; accepted 17 August 2022. Date of publication 22 August 2022; date of current version 5 January 2023. This work was supported in part by Innovation Fund Denmark. (*Corresponding author: Magnus Brandt-Møller.*)

Magnus Brandt-Møller is with TICRA, 1119 Copenhagen, Denmark, and also with the National Space Institute, Electromagnetic Systems, Technical University of Denmark, 2800 Kgs. Lyngby, Denmark (e-mail: mbm@ticra.com).

Michael Mattes is with the National Space Institute, Electromagnetic Systems, Technical University of Denmark, 2800 Kgs. Lyngby, Denmark (e-mail: mmattes@elektro.dtu.dk).

Olav Breinbjerg is with EIMaReCo, 1055 Copenhagen, Denmark (e-mail: olavbreinbjerg@outlook.com).

Min Zhou and Oscar Borries are with TICRA, 1119 Copenhagen, Denmark (e-mail: mz@ticra.com; ob@ticra.com).

Digital Object Identifier 10.1109/LAWP.2022.3200855

array of PEC spheres. Section IV investigates a DRA, demonstrating the increased efficiency using HO-BF. Finally, Section V concludes this letter.

II. ARRAY DECOMPOSITION METHOD

This section outlines the boundary integral part of ADM [14] from a matrix algebraic perspective with the purpose demonstrating its implementation. We take outset in an arbitrary volumetric antenna array of identical elements, which are placed on a d -dimensional regular lattice, and write the total number of unknowns as

$$N = s \prod_{i=1}^d n_i = sT \quad (1)$$

where s is the total number of BF (unknowns) on each array element, d is the total number of array lattice dimensions and n_i is the number of array elements in each dimension i . $T = n_1 n_2 \dots n_d$ is the total number of array elements. Due to the translation symmetry of the 3-D free-space Green function, the regular lattice on which array elements are placed, as well as consecutively ordered BF, the MoM matrix $\mathbf{A} \in \mathbb{C}^{N \times N}$ becomes multilevel (BT) of $d + 1$ levels. That is, \mathbf{A} consists of $n_1 \times n_1$ BT matrices, which themselves consist of $n_2 \times n_2$ BT subblocks, and so forth for the number of array lattice dimensions d . The last level $d + 1$ contains, in general, an asymmetric $s \times s$ square matrix containing the basis/test function interactions between the array elements.

The speed-up of ADM comes from an expedited MVP combined with an iterative solver. The core of ADM can algebraically be regarded as extending the subblocks at each level $i = 1, \dots, d$ from Toeplitz to circulant blocks [15, Sec. 4.7.7], excluding the blocks at the innermost level which, in general, do not possess any special symmetry. The extended MoM matrix \mathbf{A}^C formally increases the number of unknowns \tilde{N} as

$$\tilde{N} = s \prod_{i=1}^d (2n_i - 1) \approx 2^d N. \quad (2)$$

The additional unknowns are eventually disregarded, and are as such merely a mathematical trick to allow for the circulant extension. We note that an antenna array on a 1-, 2-, or 3-D regular lattice, results in about 2, 4, or 8 times as many unknowns, respectively. Nevertheless, as it will soon become clear, the circulant property allows for a significant reduction in both matrix storage and computational complexity.

Starting with the simpler example ($s = 1, d = 2, [n_1, n_2] = [2, 2]$), \mathbf{A}^C assumes a block-circulant with circulant-blocks structure

$$\mathbf{A}^C = \begin{bmatrix} \vec{c}^1 \left\{ \begin{array}{ccc|ccc} \underline{a_1} & \underline{a_3} & \underline{a_2} & \underline{a_7} & \underline{a_9} & \underline{a_8} & \underline{a_4} & \underline{a_6} & \underline{a_5} \\ \underline{a_2} & \underline{a_1} & \underline{a_3} & \underline{a_8} & \underline{a_7} & \underline{a_9} & \underline{a_5} & \underline{a_4} & \underline{a_6} \\ \underline{a_3} & \underline{a_2} & \underline{a_1} & \underline{a_9} & \underline{a_8} & \underline{a_7} & \underline{a_6} & \underline{a_5} & \underline{a_4} \end{array} \right. \\ \hline \vec{c}^2 \left\{ \begin{array}{ccc|ccc} \underline{a_4} & \underline{a_6} & \underline{a_5} & \underline{a_1} & \underline{a_3} & \underline{a_2} & \underline{a_7} & \underline{a_9} & \underline{a_8} \\ \underline{a_5} & \underline{a_4} & \underline{a_6} & \underline{a_2} & \underline{a_1} & \underline{a_3} & \underline{a_8} & \underline{a_7} & \underline{a_9} \\ \underline{a_6} & \underline{a_5} & \underline{a_4} & \underline{a_3} & \underline{a_2} & \underline{a_1} & \underline{a_9} & \underline{a_8} & \underline{a_7} \end{array} \right. \\ \hline \vec{c}^3 \left\{ \begin{array}{ccc|ccc} \underline{a_7} & \underline{a_9} & \underline{a_8} & \underline{a_4} & \underline{a_6} & \underline{a_5} & \underline{a_1} & \underline{a_3} & \underline{a_2} \\ \underline{a_8} & \underline{a_7} & \underline{a_9} & \underline{a_5} & \underline{a_4} & \underline{a_6} & \underline{a_2} & \underline{a_1} & \underline{a_3} \\ \underline{a_9} & \underline{a_8} & \underline{a_7} & \underline{a_6} & \underline{a_5} & \underline{a_4} & \underline{a_3} & \underline{a_2} & \underline{a_1} \end{array} \right. \end{bmatrix} \quad (3)$$

in which the entries of the original MoM matrix \mathbf{A} are marked with an underline. Since circulant matrices are uniquely defined by their first row/column, we only need to store the first columns \vec{c}^p of size $(2n_1 - 1) \times 1$ of each circulant block where $p = 1, \dots, 2n_2 - 1$ denotes the index of the circulant block at the second level. The actual number of matrix entries to store become $s^2 \prod_{i=1}^d (2n_i - 1) \approx 2^d s^2 T$, which is linear rather than quadratic in the number of array elements T , compared with the ordinary MoM.

The unique information of the extended-MoM matrix is stored in a $(d = 2)$ -dimensional matrix \mathbf{C} , which amounts to the first block columns \vec{c}^p of \mathbf{A}^C

$$\mathbf{C} = \begin{bmatrix} \vec{c}^1 & \vec{c}^2 & \vec{c}^3 \end{bmatrix} \in \mathbb{C}^{(2n_1-1) \times (2n_2-1)}. \quad (4)$$

The entries in the MVP \mathbf{V} of the circulant-extended MoM matrix \mathbf{A}^C with a given vector \vec{x} , can be expressed as a $(d = 2)$ -dimensional circular convolution

$$\mathbf{V} = \mathbf{C} \circledast \mathbf{X} \quad (5)$$

in which \mathbf{X} is a $(d = 2)$ -dimensional matrix of the same size and dimensions as \mathbf{C} in which the only nonzero elements are the original unknowns placed at the indices $\mathbf{X}_{1 \dots n_1, 1 \dots n_2}$. Through the circular convolution theorem, the $(d = 2)$ -dimensional discrete circular convolution can be expressed in terms of the discrete Fourier transformation as

$$\mathbf{V} = \mathcal{F}_2^{-1} \left\{ \mathcal{F}_2 \left\{ \begin{bmatrix} a_1 & a_4 & a_7 \\ a_2 & a_5 & a_8 \\ a_3 & a_6 & a_9 \end{bmatrix} \right\} \odot \mathcal{F}_2 \left\{ \begin{bmatrix} x_1 & x_4 & 0 \\ x_2 & x_5 & 0 \\ 0 & 0 & 0 \end{bmatrix} \right\} \right\} \quad (6)$$

where \mathcal{F}_2 denotes the 2-D discrete Fourier transform and \odot denotes the Hadamard operator, i.e., elementwise multiplication. Hereafter, the entries \mathbf{U} of the desired MVP $\vec{u} = \mathbf{A}^C \vec{x}$, is readily available by accessing the submatrix $\mathbf{U} = \mathbf{V}_{1 \dots n_1, 1 \dots n_2} \in \mathbb{C}^{n_1 \times n_2}$, after which the column vector \vec{u} is obtained by interpreting the contiguous memory column-major matrix \mathbf{U} as a 1-D vector.

In the more general case where ($s > 1, d = 2, [n_1, n_2] = [2, 2]$), the unique entries a_k of \mathbf{A}^C for $k = 1, \dots, \tilde{N}$ themselves become matrices $\mathbf{a}_k \in \mathbb{C}^{s \times s}$ with entries denoted by $a_k^{m,n}$, while the vector entries x_k become column vectors $\vec{x}_k \in \mathbb{C}^{s \times 1}$ with entries enumerated as x_k^n . Since the innermost \mathbf{a}_k blocks do not, in general, possess any special symmetry they cannot be accelerated by the FFT. Consequently, in order to obtain the full MVP entries \mathbf{V} , several MVP \mathbf{V}_m need to be computed for each $m = 1, \dots, s$ by summation of Hadamard products over $n = 1, \dots, s$, as shown in (7) at the bottom of the next page.

The desired MVP $\vec{u} = \mathbf{A}^C \vec{x}$ is obtained by copying the submatrices $\mathbf{U}_m = \mathbf{V}_m(1:n_1, 1:n_2)$ interpreted as column vectors, into \vec{u} in the order of m . Note that in practice, the Fourier transformations \mathcal{F}_2 of $\mathbf{C}^{m,n}$ for all m and n are performed only once before entering the iterative solution process, while the Fourier transformation \mathcal{F}_2 of \mathbf{X}_n and the inverse Fourier transformation \mathcal{F}_2^{-1} for \mathbf{V}_m , over all n and m , respectively, are performed only once per MVP.

In the most general case where ($s > 1, d \geq 1$), the entries \mathbf{V}_m of the MVP of the circulant-extended MoM matrix \mathbf{A}^C with a

given vector \vec{x} become

$$\mathbf{V}_m = \mathcal{F}_d^{-1} \left\{ \sum_{n=1}^s \mathcal{F}_d \{ \mathbf{C}^{m,n} \} \odot \mathcal{F}_d \{ \mathbf{X}^n \} \right\} \quad (8)$$

where \mathcal{F}_d denotes the d -dimensional discrete Fourier transform. In this general case, $\mathbf{C}^{m,n}$ becomes a d -dimensional tensor containing the entries $a_k^{m,n}$ arranged consecutively in k along the d -dimensions of size $(2n_1 - 1) \times \dots \times (2n_d - 1)$. \mathbf{X} becomes a d -dimensional tensor of the same size and dimensions in which the only nonzero elements are the original nonextended unknowns placed at the indices $\mathbf{X}_{1 \dots n_1, \dots, 1 \dots n_d}$.

In conclusion, in the general case, the computational complexity of ADM is $\mathcal{O}(s^2 T \log(T))$ rather than $\mathcal{O}(N \log N)$. Hence, it is evident that the quadratic scaling with s is a consequence of permitting a general $s \times s$ matrix at the innermost level. Consequently, it is critical to keep the number of BF, s , on each array element (i.e., unknowns at the innermost level) as low as possible without impacting the solution accuracy. This can be achieved using HO BF, as will be demonstrated in the following section.

III. HO CONVERGENCE

In this work, ADM has been implemented using the mixed-potential electric field integral equation, as well as the combined field integral equation (CFIE) for closed surfaces [12]. Curved quadrilaterals (mesh-cells) with parameterization $\vec{\mathbf{r}}(u, v)$ are used to discretize the geometry [16] using the HO hierarchical Legendre BF from [12] to expand the surface current density as

$$\begin{aligned} \vec{\mathbf{J}}(u, v) = & \frac{\vec{\mathbf{a}}_u}{\mathcal{J}_S(u, v)} \sum_{m=0}^{M^u} \tilde{P}_m(u) \sum_{n=0}^{N^v} C_{mn}^{uv} P_n(v) a_{mn}^u \\ & + \frac{\vec{\mathbf{a}}_v}{\mathcal{J}_S(u, v)} \sum_{m=0}^{M^v} \tilde{P}_m(v) \sum_{n=0}^{N^u} C_{mn}^{uv} P_n(u) a_{mn}^v \end{aligned} \quad (9)$$

in which $a_{mn}^{\{u,v\}}$ are the unknown current coefficients in the $\{u, v\}$ -direction, $\vec{\mathbf{a}}_{\{u,v\}} = \frac{\partial \vec{\mathbf{r}}}{\partial \{u,v\}}$ are covariant unitary vectors, \mathcal{J}_S is the surface Jacobian, and P_n are Legendre polynomials of order n . C_{mn}^{uv} are constants chosen to minimize the MoM matrix condition number and \tilde{P}_m are the modified Legendre polynomials

$$\tilde{P}_m(u) = \begin{cases} 1 - u & m = 0 \\ 1 + u & m = 1 \\ P_m(u) - P_{m-2}(u) & m \geq 2. \end{cases} \quad (10)$$

The value $N^{\{u,v\}} = M^{\{u,v\}} - 1$, and is the maximum polynomial order used for the current expansion in the $\{u, v\}$ -direction, which in this letter is denoted by ρ . The key benefit of employing polynomial orders $\rho > 1$ is that the discretization error behaves

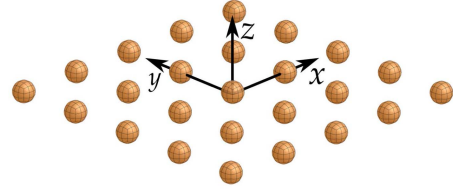


Fig. 1. 5×5 element PEC sphere array. 5λ diameter. 16λ interelement distance.

as $\mathcal{O}(h^\rho)$, where h is a relative mesh cell size [13]; that is, increasing the polynomial order ρ of employed BF theoretically yield better accuracy than increasing the mesh discretization (for the same number of unknowns). This property is customarily denoted as HO convergence, and has been verified for a single sphere for MoM [17] and MLFMM [18]. Note that in practice, the polynomial order is adjusted to the electrical size of each mesh cell, since a general rule for choosing the optimum polynomial order *a priori* is not available. In this work, we have used a fixed polynomial order on all mesh cells for the purpose of showing HO convergence.

A. Array of Spheres

To demonstrate HO convergence in HO-ADM, we consider a 5×5 array of PEC spheres (see Fig. 1) with interelement distance of $L = 16\lambda$ and diameter $D = 5\lambda$, illuminated by an \vec{x} -polarized plane wave, propagating along the z -axis. The scattered electric far-field intensity is evaluated and compared with an accurate reference solution using the total relative rms error measure (denoted far-field error)

$$\epsilon_{\text{rms}} = \sqrt{\frac{\sum_{i=1}^{N_s} |\mathbf{E}_{i,\text{ref}} - \mathbf{E}_i|^2}{\sum_{i=1}^{N_s} |\mathbf{E}_{i,\text{ref}}|^2}} \quad (11)$$

where $\mathbf{E}_{i,\text{ref}}$ is the reference electric far field, \mathbf{E}_i is the calculated electric far-field vector, and N_s is the number of far-field samples in a regular grid over the 4π far-field sphere. Because an analytical solution is not readily available, the reference is a direct solution of the full HO-MoM matrix with high integration precision and as fine a discretization as possible within memory limits.

In Fig. 2, the far-field error ϵ_{rms} for the sphere array is evaluated as a function of the discretization density $h_\lambda = \frac{N}{\Omega_\lambda}$, where Ω_λ is the total surface area in square wavelengths. For a discretization density $h_\lambda < 20$, employing higher polynomial orders $\rho > 1$ does not yield a more accurate far field. However, as the discretization density rises above $h_\lambda > 20$, a clear distinction between the curves for different polynomial orders can be made. For a discretization density $h_\lambda > 100$, the far field for $\rho = 4$ is around two orders of magnitude more accurate than the far

$$\mathbf{V}_m = \mathcal{F}_2^{-1} \left\{ \sum_{n=1}^s \mathcal{F}_2 \left\{ \underbrace{\begin{bmatrix} a_1^{m,n} & a_4^{m,n} & a_7^{m,n} \\ a_2^{m,n} & a_5^{m,n} & a_8^{m,n} \\ a_3^{m,n} & a_6^{m,n} & a_9^{m,n} \end{bmatrix}}_{\mathbf{C}^{m,n}} \right\} \odot \mathcal{F}_2 \left\{ \underbrace{\begin{bmatrix} x_1^n & x_4^n & 0 \\ x_2^n & x_5^n & 0 \\ 0 & 0 & 0 \end{bmatrix}}_{\mathbf{X}^n} \right\} \right\}. \quad (7)$$

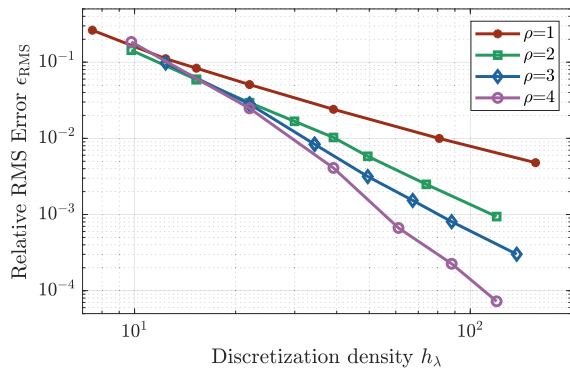


Fig. 2. Relative rms error ϵ_{rms} as a function of the discretization density h_λ (i.e., the number of unknowns normalized by total surface area in square wavelengths).

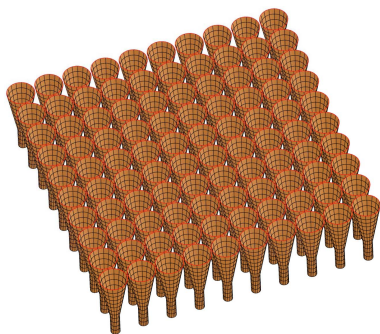


Fig. 3. 10×10 element conical horn array. 2.1λ aperture diameter. 5.6λ horn height. 2.2λ interelement distance.

field for $\rho = 1$. Moreover, for higher polynomial orders, the increasing slope of the error curves agree with the theoretical estimate $\mathcal{O}(h^\rho)$. We note that this is the first time that HO convergence has been demonstrated for an array using the ADM with hierarchical HO BF.

IV. CONICAL HORN ARRAY

As second example, we consider a $22 \times 22\lambda$ DRA (see Fig. 3), which consists of 10×10 conical horn antennas fed by circular waveguides excited uniformly with the fundamental mode TE_{11} . The radiated far-field pattern has been calculated using HO-ADM on a computer with an Intel Xeon 5218 CPU @2.3 GHz with 16 cores. A reference solution has been generated using the smallest mesh length possible on the available system. For fixed BF order ρ the maximal admissible mesh length has been varied between 0.15 and 1.5λ to ensure a relative total rms error ϵ_{rms} in the radiated far-field forward hemisphere that is less than 1% (far-field requirement).

Fig. 4 shows the total computation time (including initialization and iterative solution) and memory consumption for different BF orders ρ . For each order ρ , the maximal admissible mesh length has been decreased until reaching the far-field requirement (or lower). For $\rho = 1$, a total of 288 400 mesh cells ($\approx 0.15\lambda$) are needed to satisfy the far-field requirement, which is considerably more than the 54 000 mesh cells ($\approx 0.3\lambda$) needed for $\rho = 2$. The high number of mesh cells for $\rho = 1$ results in

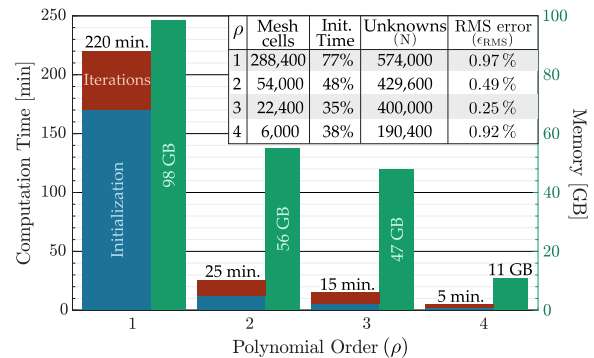


Fig. 4. Total computation time and memory consumption for HO-ADM required to reach $< 1\%$ far-field rms error.

high ADM initialization time, primarily due to the increased number of integrals to compute.

The significant reduction in computation time from 220 min ($\rho = 1$) to 25 min ($\rho = 2$) can be explained primarily by the decrease in the number of mesh cells. Notably, due to meshing constraints, the mesh is more refined for $\rho = 2$ and $\rho = 3$, resulting in a two and four times lower rms error, respectively, than the solution for $\rho = 1$ and $\rho = 4$. The increased accuracy is the primary reason for the relatively small decrease in total number of unknowns, memory consumption and computation time from $\rho = 2$ to $\rho = 3$. Nevertheless, a significant fourfold reduction in memory consumption (47 to 11 GB) and a threefold reduction in computation time (15 to 5 min) is evident going from $\rho = 3$ with 22 400 mesh cells ($\approx 0.5\lambda$) to $\rho = 4$ with 6000 mesh cells ($\approx 1.0\lambda$). Note that increasing the polynomial order above four for the present example requires a coarser mesh than possible for the given geometrical structure.

The results clearly demonstrate superior performance when increasing the BF order. This is most clearly seen going from $\rho = 1$ to $\rho = 4$, where the total computation time decreases by a factor of about 40 and the memory consumption decrease by a factor of about 10. Moreover, by increasing the polynomial order by one (from $\rho = 1$ to $\rho = 2$), the total computation time decreases by a factor of nine, the memory decreases by a factor of two, even while the rms error is halved.

V. CONCLUSION

In this contribution, the ADM and HO hierarchical BF have been combined for the first time to the best of our knowledge. The efficiency of employing HO BF to represent the surface current density has been shown for both a scattering problem (array of spheres) and a radiation problem (conical horn array), achieving HO convergence.

The results show that substantial memory savings and considerable computational speed-ups are possible by this combination while at the same time maintaining, or even improving, the accuracy. In the present test case of a 10×10 element conical horn array ($22 \times 22\lambda$), memory consumption could be reduced by a factor of up to 10 and the simulation accelerated up to 40 times, when going from first- to fourth-order BF.

REFERENCES

- [1] R. Coifman, V. Rokhlin, and S. Wandzura, "The fast multipole method for the wave equation: A pedestrian prescription," *IEEE Antennas Propag. Mag.*, vol. 35, no. 3, pp. 7–12, Jun. 1993.
- [2] C.-C. Lu and W. C. Chew, "A multilevel algorithm for solving a boundary integral equation of wave scattering," *Microw. Opt. Technol. Lett.*, vol. 7, no. 10, pp. 466–470, 1994.
- [3] B. Karaosmanoğlu and Ö. Ergül, "Acceleration of MLFMA simulations using trimmed tree structures," *IEEE Trans. Antennas Propag.*, vol. 69, no. 1, pp. 356–365, Jan. 2021.
- [4] E. Bleszynski, M. Bleszynski, and T. Jaroszewicz, "AIM: Adaptive integral method for solving large-scale electromagnetic scattering and radiation problems," *Radio Sci.*, vol. 31, no. 5, pp. 1225–1251, 1996.
- [5] S. Sharma and P. Triverio, "AIMx: An extended adaptive integral method for the fast electromagnetic modeling of complex structures," *IEEE Trans. Antennas Propag.*, vol. 69, no. 12, pp. 8603–8617, Dec. 2021.
- [6] J. White, J. Phillips, and T. Kormeyer, "Comparing precorrected-FFT and fast multipole algorithms for solving three-dimensional potential integral equations," in *Proc. Colorado Conf. Iterative Methods*, 1994, pp. 4–10.
- [7] C.-F. Wang, F. Ling, and J.-M. Jin, "A fast full-wave analysis of scattering and radiation from large finite arrays of microstrip antennas," *IEEE Trans. Antennas Propag.*, vol. 46, no. 10, pp. 1467–1474, Oct. 1998.
- [8] R. W. Kindt and J. L. Volakis, "Array decomposition-fast multipole method for finite array analysis," *Radio Sci.*, vol. 39, no. 2, pp. 1–9, 2004.
- [9] A. Geranmayeh, W. Ackermann, and T. Weiland, "FFT accelerated marching-on-in-order methods," in *Proc. 38th Eur. Microw. Conf.*, 2008, pp. 511–514.
- [10] E. H. Bleszynski, M. K. Bleszynski, and T. Jaroszewicz, "Block-Toeplitz fast integral equation solver for large finite periodic and partially periodic array systems," *IEICE Trans. Electron.*, vol. 87, no. 9, pp. 1586–1594, 2004.
- [11] R. Kindt, K. Sertel, E. Topsakal, and J. L. Volakis, "An extension of the array decomposition method for large finite-array analysis," *Microw. Opt. Technol. Lett.*, vol. 38, no. 4, pp. 323–328, 2003.
- [12] E. Jørgensen, J. L. Volakis, P. Meincke, and O. Breinbjerg, "Higher order hierarchical Legendre basis functions for electromagnetic modeling," *IEEE Trans. Antennas Propag.*, vol. 52, no. 11, pp. 2985–2995, Nov. 2004.
- [13] J.-C. Nédélec, "Mixed finite elements in R³," *Numerische Mathematik*, vol. 35, no. 3, pp. 315–341, 1980.
- [14] R. W. Kindt, K. Sertel, E. Topsakal, and J. L. Volakis, "Array decomposition method for the accurate analysis of finite arrays," *IEEE Trans. Antennas Propag.*, vol. 51, no. 6, pp. 1364–1372, Jun. 2003.
- [15] G. H. Golub and C. F. Van Loan, *Matrix Computations*. Baltimore, MD, USA: Johns Hopkins Univ., 1996.
- [16] R. D. Graglia, D. R. Wilton, and A. F. Peterson, "Higher order interpolatory vector bases for computational electromagnetics," *IEEE Trans. Antennas Propag.*, vol. 45, no. 3, pp. 329–342, Mar. 1997.
- [17] E. Jørgensen, "Higher-order integral equation methods in computational electromagnetics," Ph.D. dissertation, Ørsted-DTU, Technical Univ. Denmark, Lyngby, Denmark, 2003.
- [18] O. Borries, P. Meincke, E. Jørgensen, and P. C. Hansen, "Multilevel fast multipole method for higher order discretizations," *IEEE Trans. Antennas Propag.*, vol. 62, no. 9, pp. 4695–4705, Sep. 2014.